

The projected timing of climate departure from recent variability

Camilo Mora¹, Abby G. Frazier¹, Ryan J. Longman¹, Rachel S. Dacks², Maya M. Walton^{2,3}, Eric J. Tong^{3,4}, Joseph J. Sanchez¹, Lauren R. Kaiser¹, Yuko O. Stender^{1,3}, James M. Anderson^{2,3}, Christine M. Ambrosino^{2,3}, Iria Fernandez-Silva^{3,5}, Louise M. Giuseffi¹ & Thomas W. Giambellucca¹

Ecological and societal disruptions by modern climate change are critically determined by the time frame over which climates shift beyond historical analogues. Here we present a new index of the year when the projected mean climate of a given location moves to a state continuously outside the bounds of historical variability under alternative greenhouse gas emissions scenarios. Using 1860 to 2005 as the historical period, this index has a global mean of 2069 (± 18 years s.d.) for near-surface air temperature under an emissions stabilization scenario and 2047 (± 14 years s.d.) under a ‘business-as-usual’ scenario. Unprecedented climates will occur earliest in the tropics and among low-income countries, highlighting the vulnerability of global biodiversity and the limited governmental capacity to respond to the impacts of climate change. Our findings shed light on the urgency of mitigating greenhouse gas emissions if climates potentially harmful to biodiversity and society are to be prevented.

Climate is a primary driver of biological processes, operating from individuals to ecosystems, and affects several aspects of human life. Therefore, climates without modern precedents could cause large and potentially serious impacts on ecological and social systems^{1–5}. For instance, species whose persistence is shaped by the climate can respond by shifting their geographical ranges^{4–7}, remaining in place and adapting^{5,8}, or becoming extinct^{8–11}. Shifts in species distributions and abundances can increase the risk of extinction¹², alter community structure³ and disrupt ecological interactions and the functioning of ecosystems. Changing climates could also affect the following: human welfare, through changes in the supply of food¹³ and water^{14,15}; human health¹⁶, through wider spread of infectious vector-borne diseases^{17,18}; through heat stress¹⁹ and through mental illness²⁰; the economy, through changes in goods and services^{21,22}; and national security as a result of population shifts, heightened competition for natural resources, violent conflict and geopolitical instability²³. Although most ecological and social systems have the ability to adapt to a changing climate, the magnitude of disruption in both ecosystems and societies will be strongly determined by the time frames in which the climate will reach unprecedented states^{1,2}. Although several studies have documented the areas on Earth where unprecedented climates are likely to occur in response to ongoing greenhouse gas emissions^{24,25}, our understanding of climate change still lacks a precise indication of the time at which the climate of a given location will shift wholly outside the range of historical precedents.

To provide an indication of the projected timing of climate departure under alternative greenhouse gas emissions scenarios, we have developed an index that determines the year when the values of a given climatic variable exceed the bounds of historical variability for a particular location (Fig. 1a). We emphasize that although our index commonly identifies future dates, this does not imply that climate change is not already occurring. In fact, our index projects when ongoing climate change signals the start of a radically different climate. For this analysis we used the projections of 39 Earth System

Models developed for the Coupled Model Intercomparison Project phase 5 (CMIP5). The bounds of climate variability were quantified as the minimum and maximum values yielded by the Earth System Models with the CMIP5 ‘historical’ experiment, which for all models included the period from 1860 to 2005. This experiment included observed changes in atmospheric composition (reflecting both anthropogenic and natural sources) and was designed to model the climate’s recent past and allow the validation of model outputs against available climate observations²⁶. The year at which a climate variable moves out of the historical bounds was estimated independently with data from the Representative Concentration Pathways 4.5 (RCP45) and 8.5 (RCP85), which included the period from 2006 to 2100. These pathways or scenarios represent contrasting mitigation efforts between a concerted rapid CO₂ mitigation and a ‘business-as-usual’ scenario (CO₂ concentrations could increase to 538 and 936 p.p.m. by 2100, according to RCP45 and RCP85, respectively^{27,28}). A more aggressive mitigation scenario (RCP 2.6) was not analysed, because it was not consistently used among models, and the implicit mitigation effort is considered currently unfeasible²⁹.

We analysed five climate variables for the atmosphere and two for the oceans (Extended Data Table 1). However, we report results with mean annual near-surface air temperature as our indicator of the climate, unless otherwise specified. Simulated and actual measurements of temperature for the period 1986–2005 were remarkably similar (Extended Data Fig. 1). In comparison with any individual model’s results, the multi-model average best fitted the actual data (Extended Data Fig. 1). We therefore describe our results on the basis of multi-model averages. We show standard deviations to report the spatial variability in our results. Multi-model uncertainty (that is, the variability between models in the predicted years) was measured as the standard error of the mean, which for near-surface air temperature had a global value of 4.2 years for RCP45 and 2.7 years for RCP85 (Extended Data Fig. 2a). Multi-model uncertainty for all variables is shown in Extended Data Fig. 2.

¹Department of Geography, University of Hawai‘i at Mānoa, Honolulu, Hawai‘i 96822, USA. ²Department of Biology, University of Hawai‘i at Mānoa, Honolulu, Hawai‘i 96822, USA. ³Hawai‘i Institute of Marine Biology, University of Hawai‘i at Mānoa, Kāne‘ohe, Hawai‘i 96744, USA. ⁴Department of Oceanography, University of Hawai‘i at Mānoa, Honolulu, Hawai‘i 96822, USA. ⁵Trans-disciplinary Organization for Subtropical Island Studies (TRO-SIS), University of the Ryukyus, Senbaru, Nishihara, Okinawa 903-0213, Japan.

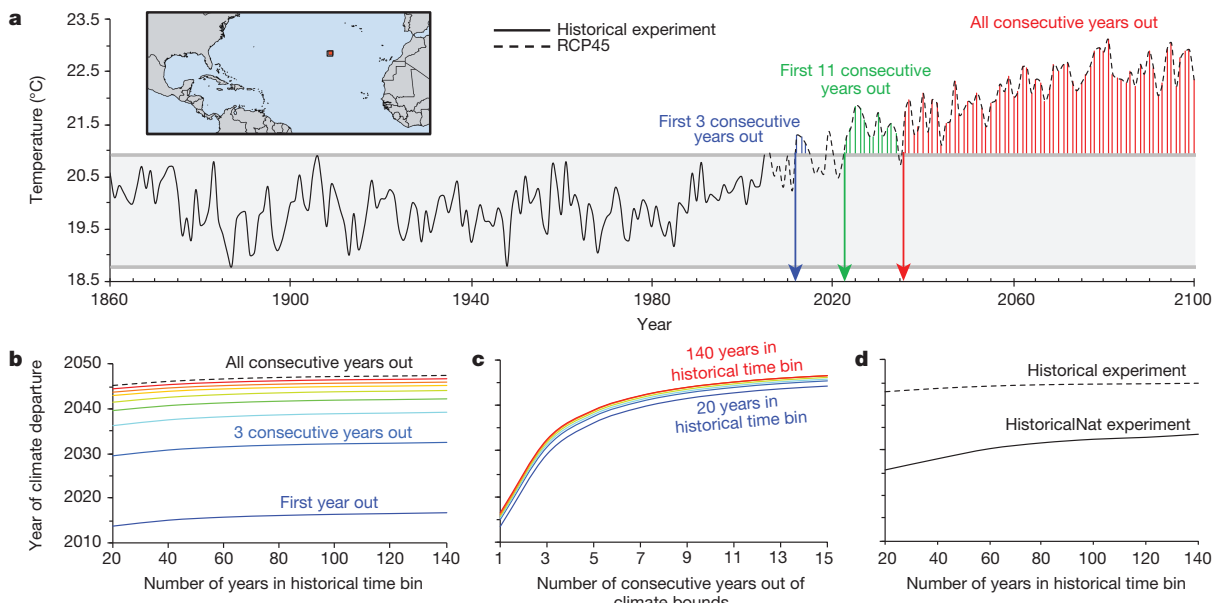


Figure 1 | Estimating the projected timing of climate departure from recent variability. **a**, Mean annual temperatures of an example grid cell (small square on map) exceed historical climate bounds (grey area) for three consecutive years starting in 2012 (blue arrow) and for 11 consecutive years after 2023 (green arrow); after 2036 (red arrow) all subsequent years remained outside the bounds (data from the Geophysical Fluid Dynamics Laboratory Earth System

Model 2G). **b, c**, Effect of using different historical reference periods (**b**) and different numbers of consecutive years exceeding historical bounds (**c**) on the projected timing of climate departure from recent variability for global multi-model averages under RCP85. **d**, Comparison of the projected timing of climate departure from recent variability under RCP85, using the ‘historical’ and the ‘historicalNat’ experiments as reference to set the bounds of historical climate variability.

Sensitivity of the index

Three factors could affect the result of our index: first, the number of years used as the historical reference period (a longer historical reference period could yield broader bounds of climate variability); second, the number of consecutive years out of historical bounds in order to declare the timing of climate departure (for example, one single year out of historical bounds will probably occur sooner than several consecutive years); and third, the extent to which the historical reference period has been affected by anthropogenic greenhouse gases (the use of a period that already contains anthropogenic effects would yield broader bounds of climate variability).

To address the first two concerns we calculated the year when the climate exceeded the bounds of historical variability, using different historical reference periods and varying numbers of consecutive years out of the historical bounds. We found that the year in which the climate exceeded the bounds of historical variability changed minimally when using historical time bins ranging from 20 to 140 years (Fig. 1b). Despite the fact that our analysis was constrained by the 140 years of available model data, the observed relationship between historical time bins (X) and the year exceeding bounds of historical climate variability (Y) showed a strong correlation for both RCPs ($Y = 1.2773 \ln X + 2063.2$ for RCP45; $Y = 1.0865 \ln X + 2042.2$ for RCP85 (dashed line in Fig. 1b); $r^2 = 0.99$ and $P < 0.001$ in both cases). Under both RCPs, extrapolating these equations from a 140-year time bin to a 1,000-year time bin increased the estimated year exceeding the bounds of historical climate variability by only about 2 years. In contrast, the year at which the climate exceeded the bounds of historical variability was sensitive to the number of consecutive years out of historical bounds considered (Fig. 1c). As illustrated for the location in Fig. 1a, the climate will experience three consecutive years out of historical bounds by 2012, 11 consecutive years by 2023, and all consecutive years after 2036. To ensure robustness in our results we used the minimum and maximum values in the entire time series of the historical experiment from 39 Earth System Models available, suggesting that our results included the broadest historical climate bounds possible, given available data. Similarly, we used the first year

after which all values would continuously exceed the bounds of historical climate variability.

To address the third concern we compared our results from the historical experiment with those obtained from an additional CMIP5 experiment, ‘historicalNat’, which simulated the same time span as the historical experiment but with only natural forcing (for example volcanoes and solar variability), while excluding anthropogenic greenhouse gas emissions²⁶. The results of this analysis (Fig. 1d) indicated that the climate surpasses the bounds of historical variability about 18.5 years earlier under RCP45, and 11.5 years earlier under RCP85 when using historical simulations that excluded anthropogenic greenhouse-gas forcing (historicalNat experiment) compared with those that included it (historical experiment). We did not use the historicalNat experiment in our main results because it was available for only 17 out of 39 Earth System Models in CMIP5 (Extended Data Table 1) and this would have sacrificed the robustness obtained by using all available models. However, the sensitivity test above provides a quantitative measure of the likely adjustment in the projected timing of climate departure if historic periods without human effects were used to quantify past climate variability, and suggests that the reported values using the historical experiment are highly conservative.

The timing of climate departure

We found that the year at which the climate exceeds the bounds of historical variability depended on the modelled scenario. Under RCP45, the projected near-surface air temperature of the average location on Earth will move beyond historical variability by 2069 (± 18 years s.d., 56 years in the future; solid blue line in Fig. 2d) and two decades earlier under RCP85 (that is, 2047 (± 14 years s.d.), 34 years in the future; solid red line in Fig. 2d). These results are sobering indicators of the pace of climate change if one considers that the timing of climate departure will occur sooner if ‘pristine’ climate conditions (that is, the historicalNat experiment) are used to set historical climate bounds: 37.5 years in the future under RCP45, or 22.5 years under RCP85. For the ocean, the historical bounds of sea surface temperature will be surpassed on average by 2072 (± 17 years s.d.) under RCP45 and by 2051 (± 16 years s.d.) under RCP85 (Extended Data Fig. 3). When the index is calculated

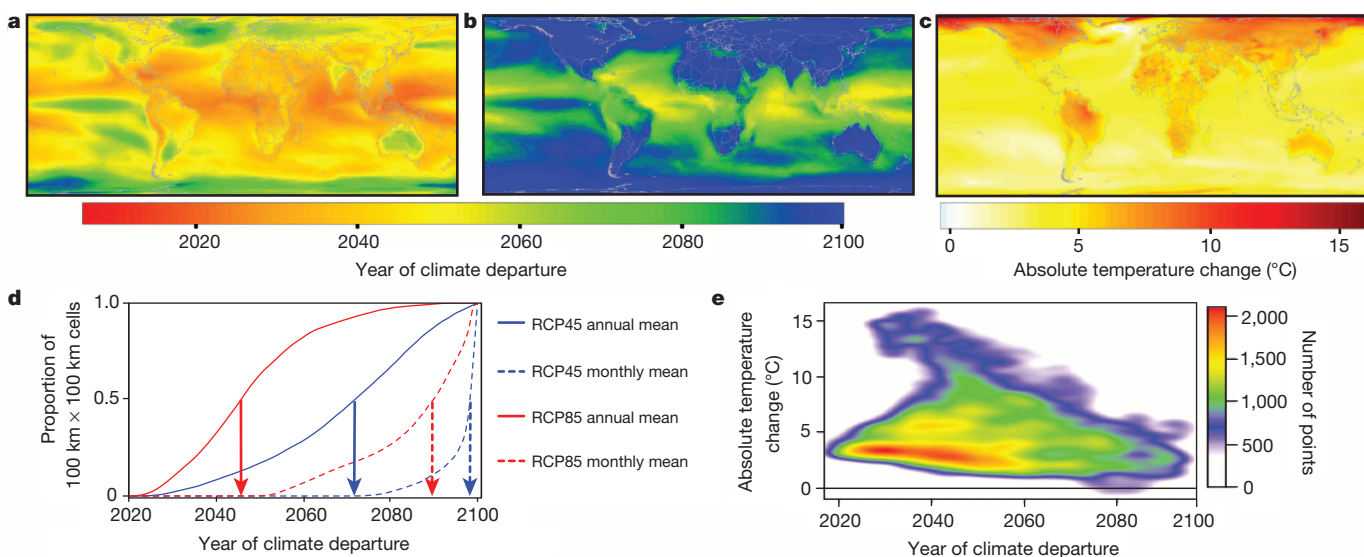


Figure 2 | The projected timing of climate departure from recent variability.

a, b, Projected year when annual (a) or monthly (b) air temperature means move to a state continuously outside annual or monthly historical bounds, respectively. c, Absolute change in mean annual air temperature. (Results in a–c are based on RCP85.) d, Cumulative frequency of 100-km grid cells

using monthly values (see Methods), all consecutive months will be out of the monthly historical bounds later in the century (Fig. 2b, dotted lines in Fig. 2d; see also Extended Data Fig. 3b, d). The estimated year when the climate exceeds historical variability is delayed when using monthly instead of annual averages, because one anomalous year is not necessarily caused by all months being extreme; thus, an anomalous year on average is likely to occur earlier than the year for which all months fall outside the monthly climate bounds. It is remarkable, however, that after 2050 most tropical regions will have every subsequent month outside of their historical range of variability (Fig. 2b). Although this is later than the yearly averages, we stress that this is an extreme situation, in which every month will be an extreme climatic record.

We used mean annual near-surface air temperature as the main proxy for the climate. However, other climate variables can change earlier or later than temperature in response to greenhouse gas emissions. To assess this effect, we analysed additional climate variables under both emissions scenarios and provided an overall climate assessment by estimating the year at which the first climate variable exceeded its historical bounds of variability. These variables included evaporation, transpiration, sensible heat flux and precipitation for the Earth's atmosphere, and surface pH for the ocean. For the atmosphere, the projected timing of climate departure did not change when considering other climate variables along with air temperature (Extended Data Fig. 4). This occurred because air temperature will experience the earliest and most sustained changes outside historical climate bounds in comparison with other atmospheric variables (that is, other atmospheric variables will continuously surpass their historical variability later than temperature; Extended Data Fig. 4). However, the projected timing of the ocean's climate departure was pushed forward to this decade when pH was considered alongside sea surface temperature. Global mean ocean pH moved outside its historical variability by 2008 (± 3 years s.d.), regardless of the emissions scenario analysed (Extended Data Fig. 4). This result, which is consistent with recent studies³⁰, is explained by the fact that ocean pH has a narrow range of historical variability and that a considerable fraction of anthropogenic CO₂ emissions has been absorbed by the ocean^{30,31}.

Timing and absolute changes in climate

Absolute changes in the climate are often the means of detecting or assessing climate change and are expected to be considerably larger at

according to the projected timing of climate departure from recent variability for air temperature under two emissions scenarios (vertical lines indicate the median year). e, Scatter plot relating the grid cells from the map of absolute change (c) to the same grid cells from the map of projected timing of climate departure (a).

higher latitudes (Fig. 2c; see also ref. 25). Measures of absolute changes in the climate have also dominated the dialogue on climate change (for example, avoiding 2 °C warming is a broadly recognized goal among scientists, policy makers and the public, because such change is forecast to generate deleterious consequences for society and the environment^{25,32}). However, we found poor spatial correlation (Fig. 2e) between the absolute change in the climate expected by the year 2100 (Fig. 2c) and the year at which the climate would surpass historical precedents (Fig. 2a); this pattern was consistent among other climate variables (Extended Data Fig. 4). This result suggests that some aspects of climate change, which may be detrimental to biodiversity, are poorly accounted for by metrics of absolute changes in the climate; and implies that global biodiversity could face a climate change 'double jeopardy' from either large absolute changes or the early arrival of unprecedented climates.

We also found that the tropics will experience the earliest emergence of historically unprecedented climates (Fig. 2a, b). This probably occurs because the relatively small natural climate variability in this region of the world generates narrow climate bounds that can be easily surpassed by relatively small climate changes. However, small but fast changes in the climate could induce considerable biological responses in the tropics, because species there are probably adapted to narrow climate bounds^{5,33–35}. This is a prime explanation for the decline in the range sizes of species towards lower latitudes (Rapoport's rule): having narrower tolerances, tropical species are largely restricted to the tropics; in comparison, the broader physiological tolerances of temperate species allow them to survive across a broader latitudinal span³³. Furthermore, empirical and theoretical studies in corals^{5,36,37}, terrestrial ectotherms³⁴ and plants and insects³⁵ show that tropical species live in areas with climates near their physiological tolerances and are therefore vulnerable to relatively small climate changes.

The earliest emergence of unprecedented climates in the tropics and the limited tolerance of tropical species to climate change are troublesome results, because most of the world's biodiversity is concentrated in the tropics (Extended Data Fig. 5; see also ref. 33). We found that, on average, the projected timing of climate departure in marine and terrestrial biodiversity hotspots (*sensu* ref. 38, the top 10% most species-rich areas on Earth where a given taxon is found) will occur one decade earlier than the global average under either emissions scenario (Fig. 3). Coral hotspots will experience the earliest

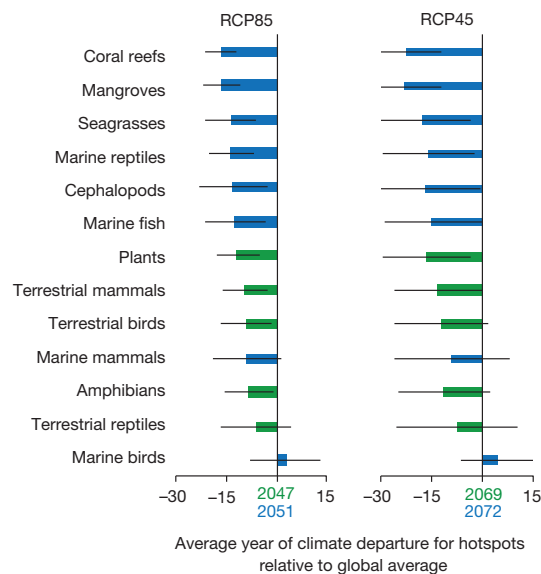


Figure 3 | The projected timing of climate departure from recent variability in global biodiversity hotspots. These plots indicate the difference between the average year in which the climate exceeds bounds of historical variability for each hotspot and the estimated global averages. The analysis was run independently for each hotspot, using mean annual air temperature for terrestrial taxa (green bars) or sea surface temperature for marine taxa (blue bars). Plots are centred at the respective global mean year for atmospheric (green numbers) and marine (blue numbers) environments. Horizontal bars rank the hotspots chronologically according to the mean year of unprecedented climates under RCP85. Horizontal black lines indicate the standard deviation among cells in the hotspots.

arrival of unprecedented climates: 2050 under RCP45 (about 23 years earlier than the global average), or 2034 under RCP85 (about 17 years earlier than the global average) (Fig. 3). With the exception of marine birds, whose hotspots are located at high latitudes (Extended Data Fig. 5d; see also ref. 39), unprecedented climates will occur at the latest by 2063 (RCP45) or 2042 (RCP85) in the hotspots of all other taxa considered (Fig. 3). Overall these results suggest that the overarching effect of climate change on biodiversity may occur not only as a result of the largest absolute changes in climate at high latitudes but also perhaps more seriously from small but prompt changes in the tropics. In short, the tropics will be highly vulnerable to climate change for at least three reasons: first, the earliest emergence of unprecedented climates will be there; second, tropical species are more vulnerable to small climate changes; and third, this region holds most of the Earth's species.

Discussion

The biological responses expected from the rapid emergence of historically unprecedented climates are likely to be idiosyncratic⁴⁰ and will depend on attributes such as species adaptive capacity, current genetic diversity, ability to migrate, current availability of habitats, disruption of ecological interactions, and ecological releases^{40–44}. Although the extent of these responses in the future has been a topic of debate^{45,46}, considerable changes in community structure³ and extinction¹⁰ have been shown to have coincided with the emergence of unprecedented climates in the past. In addition, recent short-term extreme climatic events have been associated with die-offs in terrestrial^{47–49} and marine³⁷ ecosystems, highlighting the potentially serious consequences of reaching historically unprecedented climates. Unfortunately, key conservation strategies such as protected areas, which may ameliorate the extent of several anthropogenic stressors, are unlikely to provide refuge from the expected effects of climate change, because protected areas within biodiversity hotspots will experience unprecedented climates at the same time as non-protected hotspot areas (Fig. 4a; see also ref. 50). The expansion and/or effectiveness of protected areas and other conservation

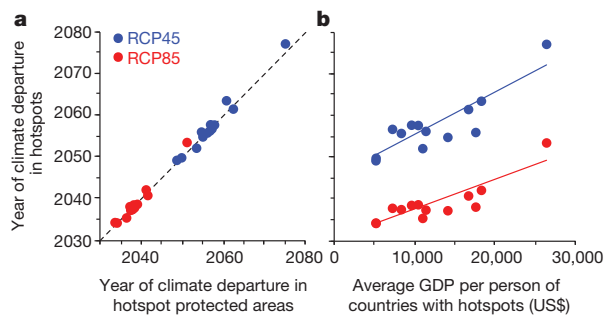


Figure 4 | Biodiversity hotspots: exposure to climate departures, and economic capacity to respond. Each point in these plots represents one of the 13 taxonomic biodiversity hotspots considered. **a**, Comparison of the year at which the climate exceeds bounds of historical variability between hotspots and protected areas in those hotspots. The dotted line shows the 1:1 relationship. **b**, Comparison of the year at which the climate exceeds bounds of historical variability in hotspots against the average Gross Domestic Product (GDP) per person for the countries encompassing the hotspots. The trend line for RCP45 is modelled with $y = 0.001x + 2045.2$ ($r^2 = 0.75$, $P < 0.05$; $n = 13$ hotspots) and for RCP85 with $y = 0.0007x + 2030.4$ ($r^2 = 0.75$, $P < 0.05$; $n = 13$ hotspots).

strategies could be further impaired by limited governmental capacity, because the earliest emergence of unprecedented climates will occur among hotspots predominantly located in low-income countries (Fig. 4b and Extended Data Fig. 6).

The emergence of unprecedented climates could also induce responses in human societies^{1,2,13–16,19–22}, and the resulting adjustments could be considerable because according to RCP45 roughly 1 billion people (about 5 billion people under RCP85) currently live in areas where climate will exceed historical bounds of variability by 2050 (Fig. 5a). The fact that the earliest climate departures occur in low-income countries (Fig. 5b) further highlights an obvious disparity between those who benefit economically from the processes leading to climate change and those who will have to pay for most of the environmental and social costs. This suggests that any progress to decrease the rate of ongoing climate change will require a bigger commitment from developed countries to decrease their emissions but will also require more extensive funding of social and conservation programmes in developing countries to minimize the impacts of climate change. Our results on the projected timing of climate departure from recent variability shed light on the urgency of mitigating greenhouse gas emissions if widespread changes in global biodiversity and human societies are to be prevented.

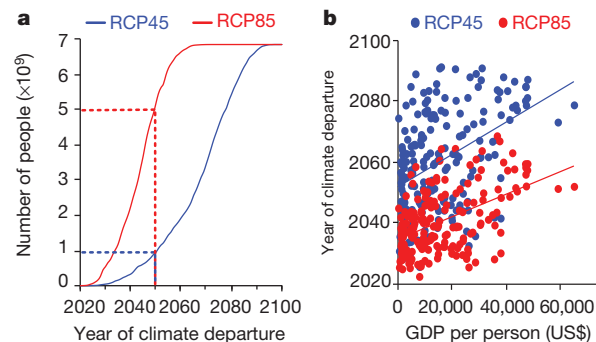


Figure 5 | Susceptibility of societies to climate departures, and economic capacity to respond. **a**, Plot of cumulative number of people against the years at which the climate of their current living areas will exceed historical climate bounds (dotted lines highlight the results for 2050). **b**, Relation between GDP per person and the average year of climate departure from recent variability. The trend line for RCP45 is modelled with $y = 0.0005x + 2051.9$ ($r^2 = 0.19$, $P < 0.05$; $n = 200$ countries or territories) and for RCP85 with $y = 0.0004x + 2034.5$ ($r^2 = 0.25$, $P < 0.05$; $n = 200$ countries or territories).

METHODS SUMMARY

We used the projections of seven climate variables (near-surface air temperature, sea surface temperature, precipitation, evaporation, transpiration, surface sensible heat flux, and ocean surface pH) from Earth System Models developed for CMIP5. As of March 2013 there were 39 Earth System Models from 21 climate centres in 12 countries that modelled at least one of the variables analysed (Extended Data Table 1). For each model and variable, we used the period 1860–2005 from the historical experiment (the longest time span common to all models), to establish the historical bounds of climate variability. The projections from RCP45 and RCP85, which simulate the period 2006–2100, were used to identify the year at which mean annual values of a given variable would exceed historical bounds. We also independently calculated the year at which the climate would exceed historical monthly variability by identifying the year containing the month after which all consecutive months, until 2100, exceeded monthly historical bounds (Fig. 2b). In total, for all variables and experiments, we processed 89,712 years of data comprising 1,076,544 monthly global maps, interpolated to an equal-area grid with a resolution of 100 km. Absolute climate change (Fig. 2c and Extended Data Figs 3c and 4) was calculated by subtracting contemporary averages (1996 to 2005) from future averages (2091 to 2100). Decadal averages were chosen to minimize aliasing by inter-annual variability. The projected timing of climate departure in biodiversity hotspots (Fig. 3), protected areas (Fig. 4), populated areas (Fig. 5a) and the economic capacity of countries (Fig. 5b) were estimated by sampling these areas from global map results on projected climate departure (based on near-surface air or sea surface temperature). All data sources are indicated in Extended Data Table 2.

Online Content Any additional Methods, Extended Data display items and Source Data are available in the online version of the paper; references unique to these sections appear only in the online paper.

Received 25 April; accepted 6 August 2013.

1. Reilly, J. & Schimmelpfennig, D. *Irreversibility, Uncertainty, and Learning: Portraits of Adaptation to Long-term Climate Change* (Springer, 2000).
2. Alley, R. B. et al. Abrupt climate change. *Science* **299**, 2005–2010 (2003).
3. Williams, J. W. & Jackson, S. T. Novel climates, no-analog communities and ecological surprises. *Front. Ecol. Environ.* **5**, 475–482 (2007).
4. Peterson, A. T., Soberon, J., Pearson, R. G. & Martinez-Meyer, E. *Ecological Niches and Geographic Distributions* (Monographs in Population Biology Vol. 49) (Princeton Univ. Press, 2011).
5. Doney, S. C. et al. Climate change impacts on marine ecosystems. *Annu. Rev. Mar. Sci.* **4**, 11–37 (2012).
6. Parmesan, C. & Yohe, G. A globally coherent fingerprint of climate change impacts across natural systems. *Nature* **421**, 37–42 (2003).
7. Chen, I.-C., Hill, J. K., Ohlemüller, R., Roy, D. B. & Thomas, C. D. Rapid range shifts of species associated with high levels of climate warming. *Science* **333**, 1024–1026 (2011).
8. Parmesan, C. Ecological and evolutionary responses to recent climate change. *Annu. Rev. Ecol. Evol. Syst.* **37**, 637–669 (2006).
9. Thomas, C. D., Franco, A. M. A. & Hill, J. K. Range retractions and extinction in the face of climate warming. *Trends Ecol. Evol.* **21**, 415–416 (2006).
10. Crowley, T. J. & North, G. R. Abrupt climate change and extinction events in Earth history. *Science* **240**, 996–1002 (1988).
11. Mora, C. & Zapata, F. A. In *The Balance of Nature and Human Impact* (ed. K. Rohde) 239–257 (Cambridge Univ. Press, 2013).
12. Berg, M. P. et al. Adapt or disperse: understanding species persistence in a changing world. *Glob. Change Biol.* **16**, 587–598 (2010).
13. Lobell, D. B. & Gourdji, S. M. The influence of climate change on global crop productivity. *Plant Physiol.* **160**, 1686–1697 (2012).
14. Zhang, X. & Cai, X. Climate change impacts on global agricultural water deficit. *Geophys. Res. Lett.* **40**, 1111–1117 (2013).
15. Taylor, R. G. et al. Ground water and climate change. *Nature Clim. Change* **3**, 322–329 (2013).
16. Patz, J. A. & Olson, S. H. Climate change and health: global to local influences on disease risk. *Ann. Trop. Med. Parasitol.* **100**, 535–549 (2006).
17. Epstein, P. R. Climate change and infectious disease: stormy weather ahead? *Epidemiology* **13**, 373–375 (2002).
18. Khasnis, A. A. & Nettleman, M. D. Global warming and infectious disease. *Arch. Med. Res.* **36**, 689–696 (2005).
19. Sherwood, S. C. & Huber, M. An adaptability limit to climate change due to heat stress. *Proc. Natl Acad. Sci. USA* **107**, 9552–9555 (2010).
20. Berry, H., Bowen, K. & Kjellstrom, T. Climate change and mental health: a causal pathways framework. *Int. J. Public Health* **55**, 123–132 (2010).
21. Diaz, S., Fargione, J., Chapin, F. S. & Tilman, D. Biodiversity loss threatens human well-being. *PLoS Biol.* **4**, e277 (2006).
22. Tol, R. S. Estimates of the damage costs of climate change. Part 1. Benchmark estimates. *Environ. Resour. Econ.* **21**, 47–73 (2002).
23. Kloot, K. The war against warming. *Nature Rep. Clim. Change* **3**, 145–146, <http://dx.doi.org/10.1038/climate.2009.120> (2009).
24. Williams, J. W., Jackson, S. T. & Kutzbach, J. E. Projected distributions of novel and disappearing climates by 2100 AD. *Proc. Natl Acad. Sci. USA* **104**, 5738–5742 (2007).
25. Solomon, S. et al. (eds). *Climate Change: The Physical Science Basis. Summary for Policymakers* (Cambridge Univ. Press, 2007).
26. Taylor, K. E., Stouffer, R. J. & Meehl, G. A. An overview of CMIP5 and the experiment design. *Bull. Am. Meteorol. Soc.* **93**, 485–498 (2012).
27. Vuuren, D. P. et al. The representative concentration pathways: an overview. *Clim. Change* **109**, 5–31 (2011).
28. Meinshausen, M. et al. The RCP greenhouse gas concentrations and their extensions from 1765 to 2300. *Clim. Change* **109**, 213–241 (2011).
29. van Vliet, J., den Elzen, M. G. & van Vuuren, D. P. Meeting radiative forcing targets under delayed participation. *Energy Econ.* **31**, S152–S162 (2009).
30. Raven, J. A. et al. (eds). *Ocean Acidification due to Increasing Atmospheric Carbon Dioxide* (Royal Society, 2005).
31. Zeebe, R. E., Zachos, J. C., Caldeira, K. & Tyrrell, T. Carbon emissions and acidification. *Science* **321**, 51–52 (2008).
32. Rockstrom, J. et al. A safe operating space for humanity. *Nature* **461**, 472–475 (2009).
33. Gaston, K. J. Global patterns in biodiversity. *Nature* **405**, 220–227 (2000).
34. Deutsch, C. A. et al. Impacts of climate warming on terrestrial ectotherms across latitude. *Proc. Natl Acad. Sci. USA* **105**, 6668–6672 (2008).
35. Colwell, R. K., Brehm, G., Cardelús, C. L., Gilman, A. C. & Longino, J. T. Global warming, elevational range shifts, and lowland biotic attrition in the wet tropics. *Science* **322**, 258–261 (2008).
36. Hoegh-Guldberg, O. Climate change, coral bleaching and the future of the world's coral reefs. *Mar. Freshw. Res.* **50**, 839–866 (1999).
37. Baker, A. C., Glynn, P. W. & Riegl, B. Climate change and coral reef bleaching: An ecological assessment of long-term impacts, recovery trends and future outlook. *Estuar. Coast. Shelf Sci.* **80**, 435–471 (2008).
38. Tittensor, D. P. et al. Global patterns and predictors of marine biodiversity across taxa. *Nature* **466**, 1098–1101 (2010).
39. Chown, S. L., Gaston, K. J. & Williams, P. H. Global patterns in species richness of pelagic seabirds: the Procellariiformes. *Ecography* **21**, 342–350 (1998).
40. La Sorte, F. A. & Jetz, W. Tracking of climatic niche boundaries under recent climate change. *J. Anim. Ecol.* **81**, 914–925 (2012).
41. Sorte, C. J. B. Predicting persistence in a changing climate: flow direction and limitations to redistribution. *Oikos* **122**, 161–170 (2013).
42. Devictor, V. et al. Differences in the climatic debts of birds and butterflies at a continental scale. *Nature Clim. Change* **2**, 121–124 (2012).
43. Zhu, K., Woodall, C. W. & Clark, J. S. Failure to migrate: lack of tree range expansion in response to climate change. *Glob. Change Biol.* **18**, 1042–1052 (2012).
44. Angert, A. L. et al. Do species' traits predict recent shifts at expanding range edges? *Ecol. Lett.* **14**, 677–689 (2011).
45. Baird, A. & Maynard, J. A. Coral adaptation in the face of climate change. *Science* **320**, 315–316 (2008).
46. Pandolfi, J. M., Connolly, S. R., Marshall, D. J. & Cohen, A. L. Projecting coral reef futures under global warming and ocean acidification. *Science* **333**, 418–422 (2011).
47. Allen, C. D. et al. A global overview of drought and heat-induced tree mortality reveals emerging climate risks for forests. *For. Ecol. Manage.* **259**, 660–684 (2010).
48. Carey, C. & Alexander, M. A. Climate change and amphibian declines: is there a link? *Divers. Distrib.* **9**, 111–121 (2003).
49. McKechnie, A. E. & Wolf, B. O. Climate change increases the likelihood of catastrophic avian mortality events during extreme heat waves. *Biol. Lett.* **6**, 253–256 (2010).
50. Mora, C. & Sale, P. Ongoing global biodiversity loss and the need to move beyond protected areas: a review of the technical and practical shortcomings of protected areas on land and sea. *Mar. Ecol. Prog. Ser.* **434**, 251–266 (2011).

Acknowledgements We thank D. Beilman for commenting on the paper; E. Wingert for help on the figures; D. Olsen for technical support; H. Kreft and the International Union for Conservation of Nature, BirdLife International, the Food and Agriculture Organization of the United Nations, the World Bank Database, the National Centers for Environmental Prediction, the World Database of Protected Areas, and the Gridded Human Population of the World Database for making their data openly available. We acknowledge the World Climate Research Programme's Working Group on Coupled Modelling, which is responsible for CMIP5, and we thank the climate modelling groups (listed in Extended Data Table 1) for producing and making available their model outputs. This work was made possible by funding from the University of Hawai'i Sea Grant to C.M. The paper was developed as part of the graduate course on 'Methods for Large Scale Analyses' in the Department of Geography, University of Hawai'i at Mānoa. A.G.F. and T.W.G. were supported by Pacific Islands Climate Change Cooperative (PICCC) award F10AC00077 and National Science Foundation Hawai'i EPSCoR grant no. EPS-0903833. R.J.L. was supported by the Pacific Islands Climate Science Center and PICCC award F10A00079. R.S.D. and E.J.T. were supported by National Science Foundation Graduate Fellowships, and I.F.-S. by a postdoctoral fellowship from the Japanese Society for the Promotion of Science.

Author Contributions All authors contributed equally to conceive the study, compile the data, conduct analyses, and write the manuscript.

Author Information Reprints and permissions information is available at www.nature.com/reprints. The authors declare no competing financial interests. Readers are welcome to comment on the online version of the paper. Correspondence and requests for materials should be addressed to C.M. (cmora@hawaii.edu).

METHODS

Approach. We used the projections of seven climatic variables (near-surface air temperature, sea surface temperature, precipitation, evaporation, transpiration, surface sensible heat flux, and ocean surface pH) from Earth System Models developed for CMIP5 (link to data source is provided in Extended Data Table 2). As of March 2013, there were 39 Earth System Models from 21 climate centres in 12 countries that modelled at least one of the variables analysed (Extended Data Table 1). We used the period 1860–2005 from the historical experiment (the longest time span common to all models) to establish the historical bounds of climate variability. The projections from RCP45 and RCP85, which simulate the period 2006–2100, were used to identify the year at which mean annual values of a given variable would exceed historical bounds (Fig. 1a). We also independently calculated the year at which the climate would exceed historical monthly variability by identifying the year containing the month after which all consecutive months, until 2100, exceeded monthly historical bounds. We used models that provided the complete data sets for the historical, RCP45 and RCP85 experiments. In total, for all variables and projections, we processed 89,712 years of data comprising 1,076,544 monthly global maps. Given that the CMIP5 models use different spatial grids to provide their data, we interpolated data from all models to an equal-area grid with a resolution of 100 km, using an area-weighted average interpolation method in which the data from the models' grid were transferred to our grid proportionally to the area that they occupied on our grid cells.

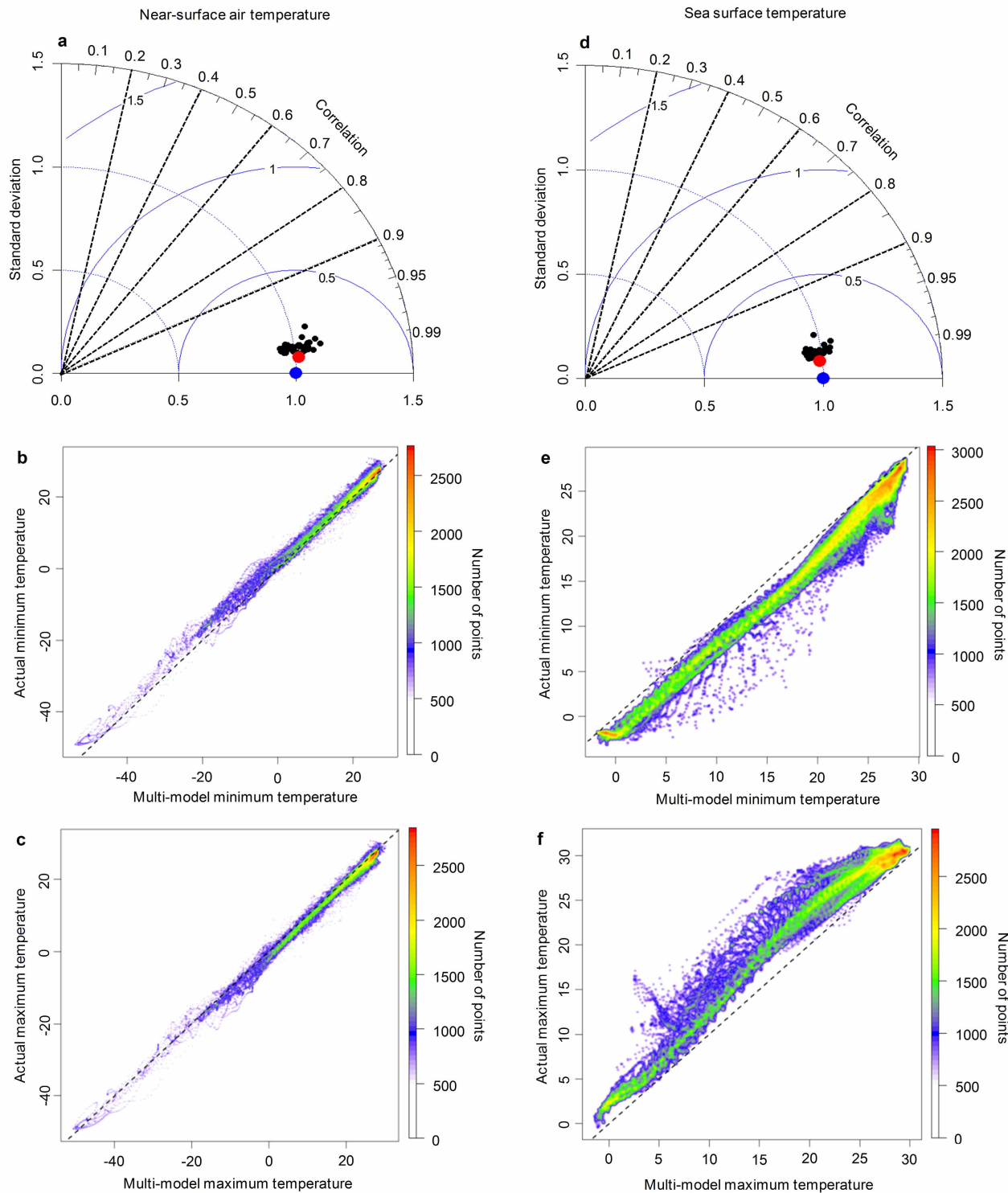
Sensitivity tests. We assessed three factors that could affect the result of our index: first, the number of years used as the historical reference period; second, the number of consecutive years out of historical bounds in order to declare the departure of climate; and third, the extent to which the historical reference period has been affected by anthropogenic greenhouse gases. To address these concerns we calculated the year when the climate exceeded the bounds of historical variability by using historical time bins varying from 20 to 140 years, by varying the number of consecutive years out of the historical bounds, and by comparing our results from the historical experiment with those obtained from an additional CMIP5 experiment, 'historicalNat', which simulated the same time span as the historical experiment, but with only natural forcing. On the basis of the results from these tests we decided to use, first, the minimum and maximum values of the entire historical period; second, the year after which all values were outside climate bounds, as our index; and third, the historical experiment as our reference period of climate variability, because it was available for all models in CMIP5 as opposed to the historicalNat experiment, which was available for only 17 out of 39

models. The test of our third concern, however, provides a measure of the difference in the results of our index using the historical reference period with human effects (historical experiment) compared with a historical reference period without human effects.

Determining the exposure of biodiversity and human societies. Biodiversity hotspots were outlined for 13 different marine (birds, cephalopods, corals, mammals, mangroves, marine fishes, reptiles and sea grasses) and terrestrial (amphibians, birds, mammals, reptiles and plants) taxonomic groups from global patterns of species richness (data sources are provided in Extended Data Table 2). Biodiversity hotspots were defined as the top 10% most species-rich areas on Earth where a given taxon is found (*sensu* ref. 33); their spatial distributions are outlined in Extended Data Fig. 5. We determined the exposure of global biodiversity hotspots to the projected timing of climate departure by intersecting biodiversity maps with maps of our index, and extracted the values in the overlapping cells. To assess the conservation potential of protected areas in biodiversity hotspots, we obtained data on protected areas, extracted all those in biodiversity hotspots and overlapped them with maps of our index to determine their timing of climate departure. We followed the same procedure for maps of population estimates and for GDP per person by country to assess the exposure of human societies and nations' economic capacities to the timing of climate departure (data sources are provided in Extended Data Table 2).

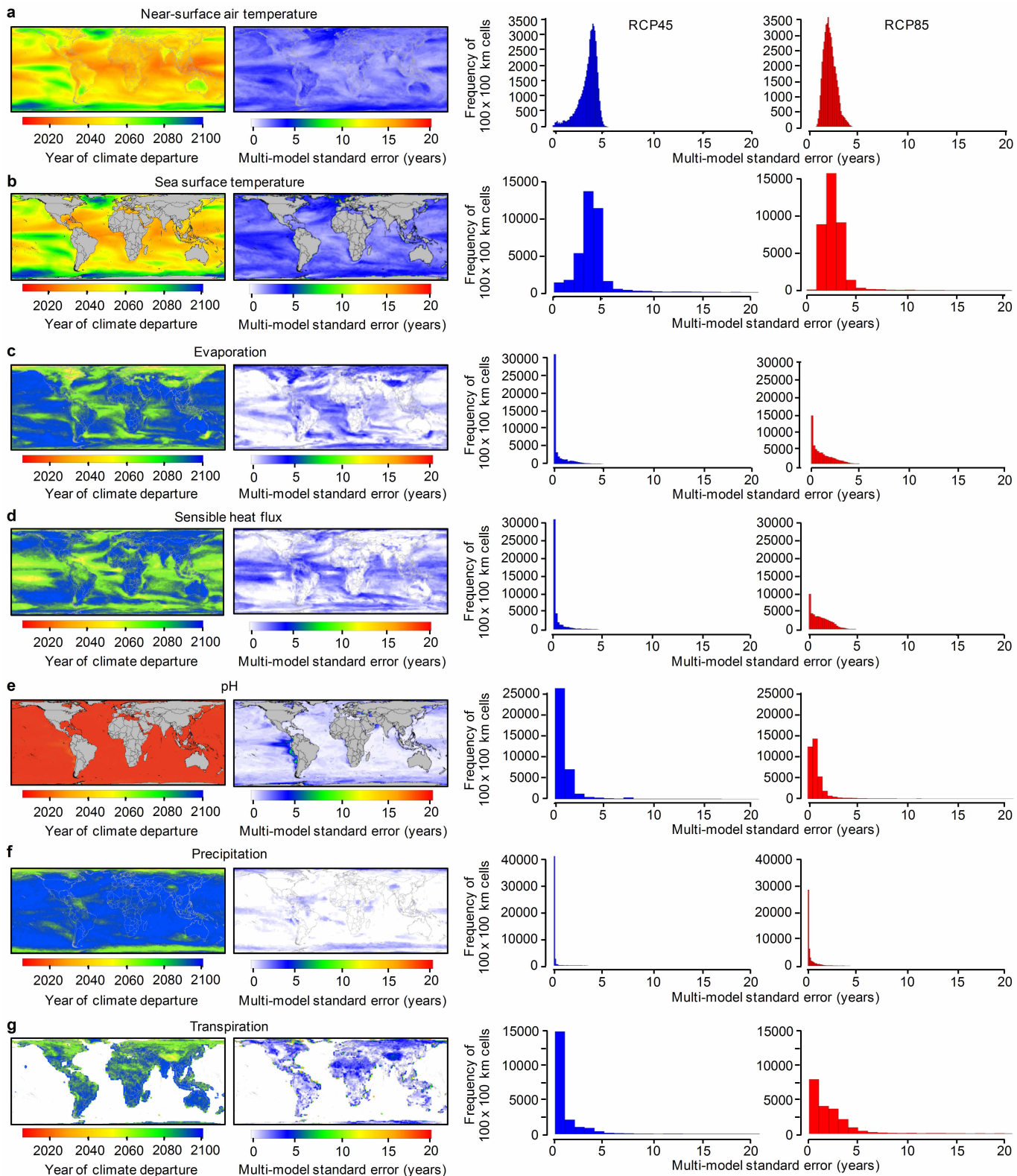
CMIP5 model robustness. We tested the robustness of CMIP5 Earth System Models by relating the simulated values and the multi-model average of near-surface air temperature and sea surface temperature from each model's output to 20 years of temperature observations (data sources are provided in Extended Data Table 2). We compared only air and sea surface temperature because of the broad availability and reliability of temperature observations. This comparison was restricted to the period 1986–2005, given the availability of actual data. The resulting metrics of fit include the correlation, the ratio of the standard deviations and the root mean squared error (all shown in Taylor diagrams in Extended Data Fig. 1a, d). Given our interest in historical climate bounds set by minimum and maximum climate values, we also compared the multi-model minimum and maximum projected values of temperature against actual minimum and maximum temperatures for the period 1986–2005 (Extended Data Fig. 1b, c, e, f).

51. Kier, G. *et al.* A global assessment of endemism and species richness across island and mainland regions. *Proc. Natl Acad. Sci. USA* **106**, 9322–9327 (2009).



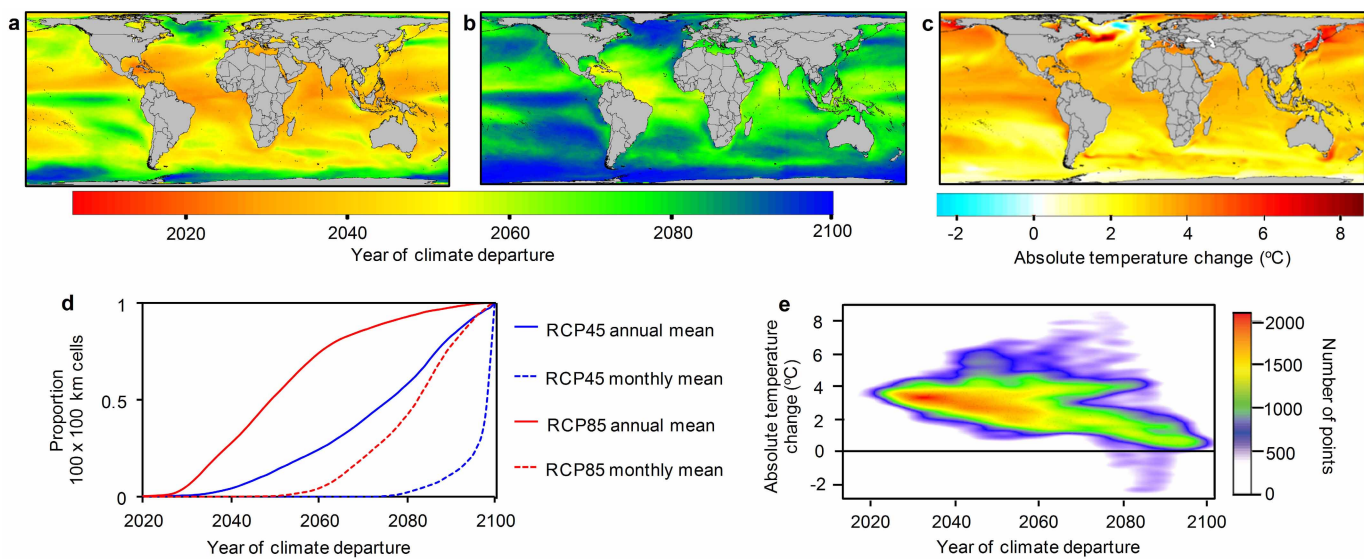
Extended Data Figure 1 | Evaluating robustness of Earth System Models.
a–c, Analysis of near-surface air temperature. **d–f**, Analysis of sea surface temperature. **a, d**, Normalized Taylor diagrams. The Taylor diagrams compare actual observations with CMIP5 model simulations, and summarize three different metrics of similitude: the correlation (curved axis), the ratio of the standard deviations (x and y axes) and the root mean squared error (blue arcs). Blue points indicate perfect fit, red points the multi-model average, and black

points the comparison of each Earth System Model to actual observations. The closer a red or black point is to the blue point, the better the fit between actual and simulated data. **b, c, e, f**, Comparison between actual and multi-model minimum (**b, e**) and maximum (**c, f**) temperatures for the 20-year period 1986–2005 (the time frame for which actual observations were mostly available). Dashed lines indicate the 1:1 relationship.



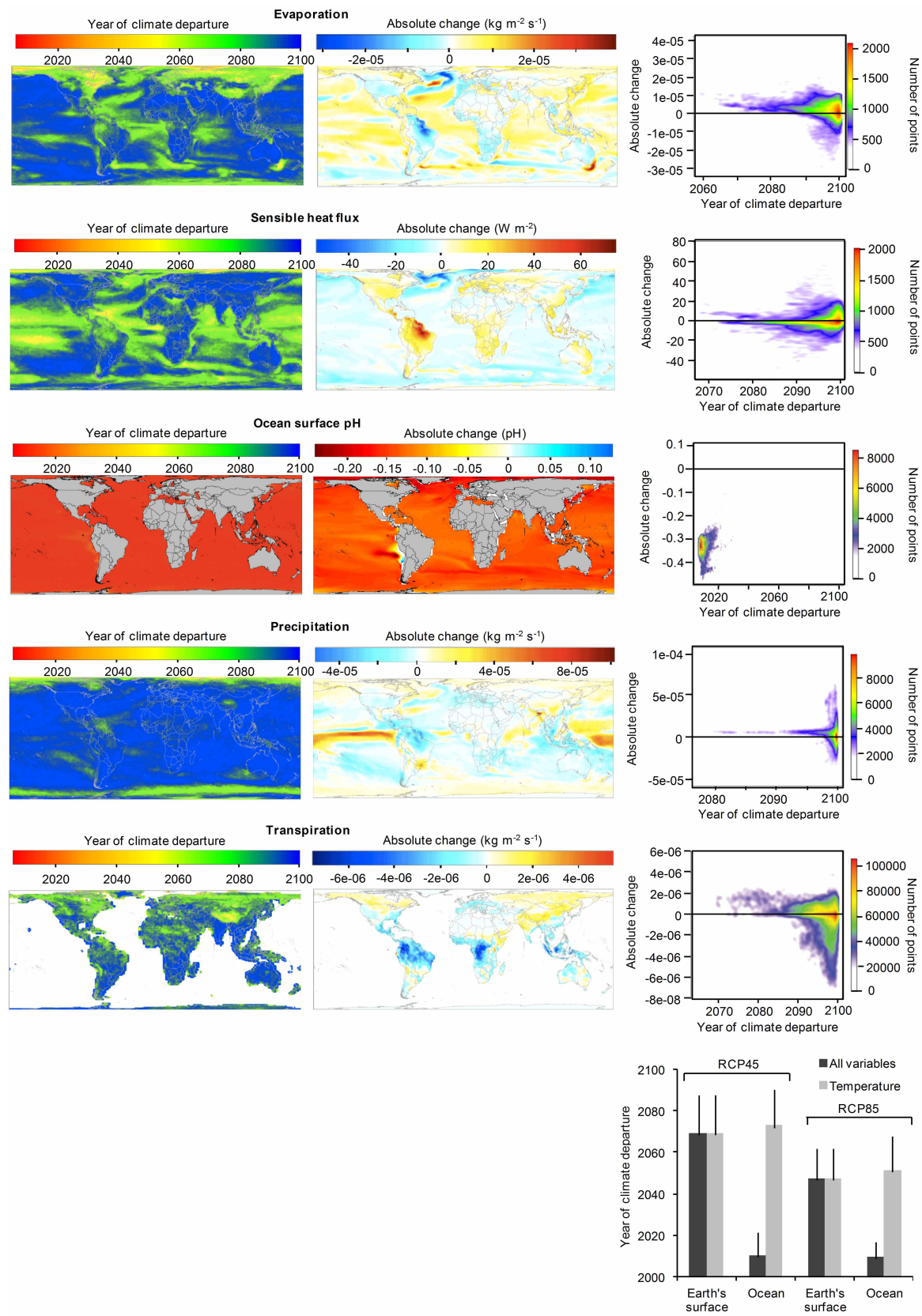
Extended Data Figure 2 | Multi-model uncertainty in the projected timing of climate departure. Results are shown for near-surface air temperature (a), sea surface temperature (b), evaporation (c), sensible heat flux (d), ocean surface pH (e), precipitation (f) and transpiration (g). Maps on the left show the mean year of climate departure under RCP85, and maps on the right illustrate the spatial patterns of inter-model standard error of the mean for RCP85. The histograms on the right indicate the frequency of grid cells by multi-model standard error of the mean according to each emissions scenario (blue, RCP45; red, RCP85).

the spatial patterns of inter-model standard error of the mean for RCP85. The histograms on the right indicate the frequency of grid cells by multi-model standard error of the mean according to each emissions scenario (blue, RCP45; red, RCP85).



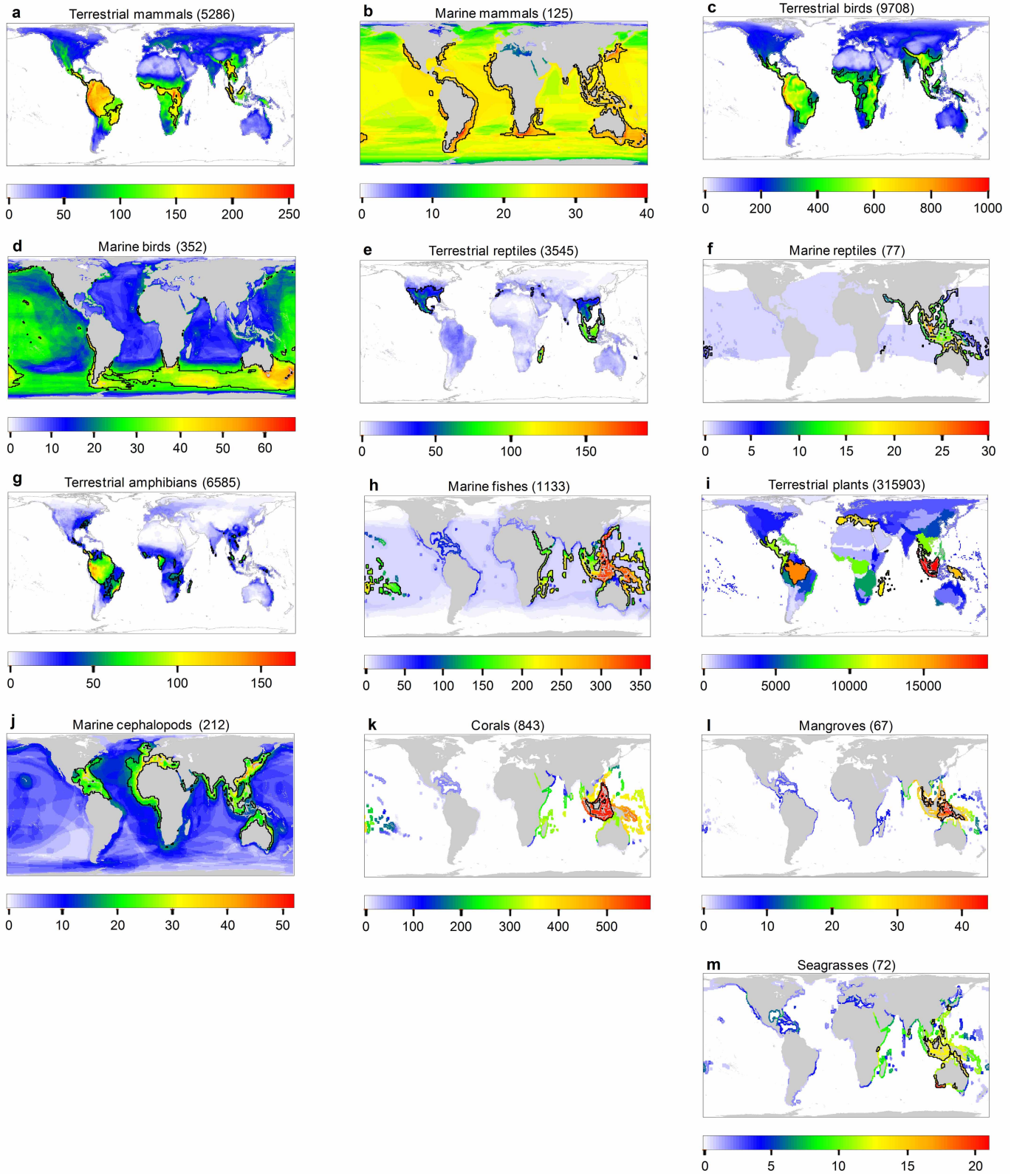
Extended Data Figure 3 | Sea surface temperature and projected timing of climate departure. **a, b**, Projected year when annual (**a**) or monthly (**b**) sea surface temperature means move to a state continuously outside annual or monthly historical bounds, respectively. **c**, Absolute change in mean annual sea surface temperature. (Results in **a–c** are based on RCP85.) **d**, Cumulative

frequency of 100-km resolution grid cells according to the year of climate departure under the two emissions scenarios and for mean annual and monthly sea surface temperature. **e**, Scatter plot relating the grid cells from the absolute change map (**c**) to the same grid cells from the projected timing of climate departure map (**a**).



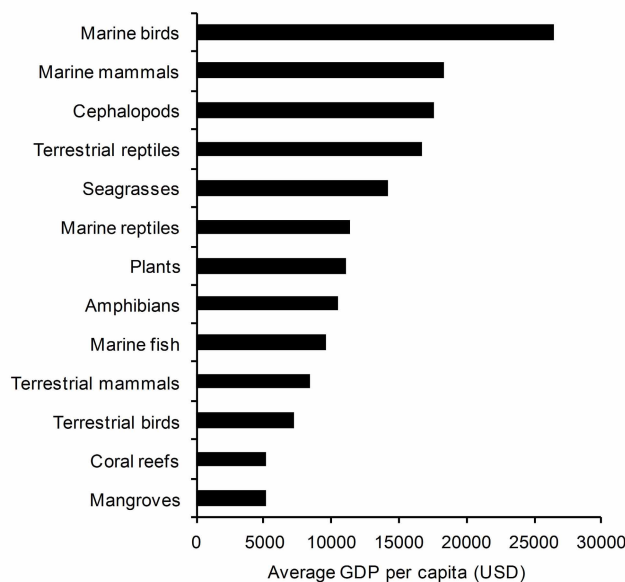
Extended Data Figure 4 | Projected timing of climate departure for different climate variables. We calculated the year of climate departure for five variables in addition to temperature. We considered the year of climate departure as the year at which the first variable exceeded its historical bounds of variability. The plots show the year of climate departure (left), the absolute

change (middle) and the relation between the departure year and absolute change (right) under RCP85. The plot at the bottom right compares the global average year using temperature alone with the year when considering additional climate variables. Vertical lines indicate s.d.



Extended Data Figure 5 | Biodiversity hotspots. Global patterns of species richness were mapped for 13 marine and terrestrial taxa. For each taxon, we outlined biodiversity hotspots as the top 10% most species-rich places on Earth where the given taxon occurred (bold black lines). For mammals, birds, reptiles, amphibians, marine fishes, cephalopods, corals, mangroves and seagrasses (a-h, j-m), we used expert-verified geographical ranges to map patterns of

species richness by counting the number of species whose ranges overlapped with an equal-area grid with a resolution of 100 km. i, For terrestrial vascular plants we used the number of species in different regions (data from ref. 51) and calculated species richness as the highest number of species occurring in the regions intersecting each 100-km resolution grid cell. The number of species or species richness used for each taxonomic group is indicated in parentheses.



Extended Data Figure 6 | Average gross domestic product (US\$) per person for countries where the world's biodiversity hotspots are located. Horizontal bars represent the average GDP per person for the countries containing the hotspots for the 13 taxa examined.

Extended Data Table 1 | Earth System Models analysed

CENTER	COUNTRY	MODEL	tas	evpsbl	hfss	pr	tran	thetao	ph
Beijing Climate Center, China Meteorological Administration	China	BCC-CSM1.1*	✓	✓	✓	✓	✓	✓	✓
		BCC-CSM1.1(m)	✓	✓	✓	✓	✓	✓	✓
Canadian Centre for Climate Modelling and Analysis	Canada	CanESM2*	✓	✓	✓	✓	✓	✓	✓
Centro Euro-Mediterraneo per i Cambiamenti Climatici	Italy	CMCC-CM	✓	✓	✓	✓		✓	
		CMCC-CMS	✓		✓	✓		✓	
Centre National de Recherches Météorologiques/Centre Européen de Recherche et Formation Avancée en Calcul Scientifique	France	CNRM-CM5*	✓	✓	✓	✓	✓	✓	
Commonwealth Scientific and Industrial Research Organization and Bureau of Meteorology	Australia	Access1.0	✓	✓	✓	✓		✓	
		Access1.3	✓	✓	✓	✓		✓	
Commonwealth Scientific and Industrial Research Organization with Queensland Climate Change Centre of Excellence	Australia	CSIRO-M3k3.6.0*	✓	✓	✓	✓		✓	
EC-EARTH Consortium	Europe	EC-EARTH	✓	✓	✓	✓		✓	
First Institute of Oceanography	China	FIO-ESM	✓	✓	✓	✓	✓	✓	✓
College of Global Change and Earth System Science, Beijing Normal Univ.	China	BNU-ESM*	✓	✓	✓	✓	✓	✓	✓
Institute for Numerical Mathematics	Russia	INM-CM4	✓	✓	✓	✓	✓	✓	✓
Institut Pierre-Simon Laplace	France	IPSL-CM5A-LR*	✓	✓	✓	✓	✓	✓	✓
		IPSL-CM5A-MR*	✓	✓	✓	✓	✓	✓	✓
		IPSL-CM5B-LR	✓	✓	✓	✓	✓	✓	✓
Laboratory for Atmospheric Sciences and Geophysical Fluid Dynamics and CESS Tsinghua University	China	FGOALS-g2	✓	✓	✓	✓		✓	
Laboratory for Atmospheric Sciences and Geophysical Fluid Dynamic, Chinese Academy of Sciences	China	FGOALS-s2			✓			✓	
Atmosphere and Ocean Research Institute (The University of Tokyo), National Institute for Environmental Studies, and Japan Agency for Marine-Earth Science and Technology	Japan	MIROC5	✓	✓	✓	✓	✓	✓	
Japan Agency for Marine-Earth Science and Technology, Atmosphere and	Japan	MIROC-ESM*	✓	✓	✓	✓	✓	✓	
Ocean Research Institute and National Institute for Environmental Studies		MIROC-ESM-CHEM*	✓	✓	✓	✓	✓	✓	
Met Office Hadley Centre	UK	HadCM3				✓			
		HadGEM2-CC	✓	✓	✓	✓		✓	✓
		HadGEM2-ES*	✓	✓	✓	✓		✓	✓
Max Planck Institut für Meteorologie	Germany	MPI-ESM-LR	✓	✓	✓	✓	✓	✓	✓
		MPI-ESM-MR	✓	✓	✓	✓	✓	✓	✓
Meteorological Research Institute	Japan	MRI-CGCM3*	✓	✓	✓	✓	✓	✓	
NASA Goddard Institute for Space Studies	United States	GISS-E2-H*	✓	✓	✓	✓	✓	✓	
		GISS-E2-R*	✓	✓	✓	✓	✓	✓	
National Center for Atmospheric Research	United States	CCSM4*	✓	✓	✓	✓	✓	✓	
Norwegian Climate Centre	Norway	NorESM1-M*	✓	✓	✓	✓	✓	✓	
		NorESM1-ME	✓	✓	✓	✓	✓	✓	
National Institute of Meteorological Research/Korea Meteorological Administration	Korea	HadGEM2-AO	✓		✓	✓		✓	
NOAA Geophysical Fluid Dynamics Laboratory	United States	GFDL-CM3*	✓	✓	✓	✓	✓	✓	
		GFDL-ESM2G	✓	✓	✓	✓	✓	✓	
		GFDL-ESM2M*	✓	✓	✓	✓	✓	✓	
National Science Foundation	United States	CESM1(BGC)	✓	✓	✓	✓	✓	✓	
		CESM1(CAM5)	✓	✓	✓	✓	✓	✓	
		CESM1(WACCM)	✓	✓	✓	✓	✓	✓	

The table shows the list of models used for each variable analysed. We considered only models that provided the complete series of data from 1860 to 2100 under the historical, RCP45 and RCP85 experiments; asterisks indicate that the model also provided results for the 'historicalNat' experiment (data source shown in Extended Data Table 2). The variables analysed included near-surface air temperature (CMIP5 variable name 'tas', in K), precipitation ('pr', kg m⁻² s⁻¹), evaporation ('evpsbl', kg m⁻² s⁻¹), transpiration ('tran', kg m⁻² s⁻¹), surface upward sensible heat flux ('hfss', W m⁻²), surface sea water potential temperature ('thetao', K) and pH ('ph', mol H kg⁻¹).

Extended Data Table 2 | Data sources

AGENCY	SOURCE
Earth System Models Data	
World Climate Research Programme*	http://cmip-pcmdi.llnl.gov/cmip5/availability.html
Biodiversity Data	
<i>Expert verified ranges</i>	
BirdLife International and NatureServe 2011	www.birdlife.org/
International Union for Conservation of Nature 2012	http://www.iucnredlist.org/technical-documents/spatial-data
Food and Agriculture Organization of the United Nations 2005	www.fao.org
<i>Species richness</i>	
Kier et al.	Kier G, Kreft H, Lee TM, Jetz W, Ibisch PL, Nowicki C, Mutke J, Barthlott W (2009) A global assessment of endemism and species richness across island and mainland regions. <i>Proceedings of the National Academy of Sciences</i> , 106(23): 9322-9327.
Protected Areas	
World Database on Protected Areas	http://protectedplanet.net/
Gridded Observational Data	
NOAA Earth System Research Laboratory	http://www.esrl.noaa.gov/psd/data/gridded/data.ncep.reanalysis.html http://www.esri.noaa.gov/psd/cgi-bin/db_search/DBSearch.pl?Dataset=NCEP+GODAS
Socio-Economic Data	
Gridded Human Population of the World Database	http://sedac.ciesin.columbia.edu/data/collection/qpw-v3
World Bank Database	http://data.worldbank.org/

* We acknowledge the World Climate Research Programme's Working Group on Coupled Modelling, which is responsible for CMIP5, and we thank the climate modeling groups (listed in Table S1 of this paper) for producing and making available their model output. For CMIP the U.S. Department of Energy's Program for Climate Model Diagnosis and Intercomparison provides coordinating support and led development of software infrastructure in partnership with the Global Organization for Earth System Science Portals.